

## Performance Analysis of MC-UPQC Using Artificial Intelligence

**B. Rajani, Dr. P. Sangameswara Raju**

<sup>1</sup>Research Scholar, S.V. University. College of Engineering, Dept.of Electrical Engg Tirupathi A.P INDIA  
<sup>2</sup> Professor, SV University, Tirupathi, Andhra Pradesh, INDIA

### ABSTRACT

Abstract:- The paper Emphasized on the design operation and control of Multi Converter Unified Power Quality Conditioner (MC-UPQC). The system is extended by adding a series VSC in an adjacent feeder. The device is connected between two or more feeders coming from different substations.

The use of combined system of series and shunt converters in one of the many solutions like MC-UPQC is to minimize any type of current and voltage fluctuations like voltage swell, voltage sag, power factor corrections and to compensate the supply voltage and the load current imperfections in power distribution network. The control strategies used here for controlling the MC-UPQC are dq-method and p-q theory with elaborate mathematical modeling in detail are discussed. This paper presents an Artificial Intelligence methods based approach to mitigate harmonics and has been estimated using MATLAB/SIMULINK Software.

**Keywords:** Power quality (PQ), MATLAB/SIMULATION, Multi converter - unified power quality conditioner, (MC-UPQC), voltage- source converter (VSC),Fuzzy, Neuro-Fuzzy controller(NFC).

### INTRODUCTION

Increased use of nonlinear loads by both electric utilities and end users has been affecting the quality of electric power, by causing major power quality disturbances in the distribution system such as voltage and current harmonics, imbalances, voltage flicker, voltage sag/swell and voltage interruptions etc. To eliminate these problems and to improve the power quality this paper presents a new Unified Power Quality Conditioning system called Multi Converter Unified Power Quality Conditioner (MC-UPQC). The MC-UPQC having three VSCs connected back to-back by a dc link is to compensate both current and voltage imperfections in one feeder and voltage imperfections in another feeder. This paper also presents a novel structure for a three phase four-wire (3P4W) distribution system utilizing MC-UPQC. The 3P4W system is realized from a three-phase three-wire system where the neutral of series transformer used in series part MC-UPQC is considered as the fourth wire for the 3P4W system. A new control strategy to balance the unbalanced load currents is also presented in this paper. The neutral current that may flow toward transformer neutral point is compensated by using a four-leg voltage source inverter topology for shunt part. Thus, the series transformer neutral will be at virtual zero potential during all operating conditions. The simulation results based on MATLAB/SIMULINK are presented to show the effectiveness of the proposed MC-UPQC-based 3P4W distribution system. The present work study the compensation principle and different controllers like PI, FUZZY & Neuro-Fuzzy controller of the MC-UPQC in detail. Are focused in the paper and are used in removing the problem of Neutral currents.

The nonlinear unbalanced loads leads to the problem of excessive neutral current in Three-Phase four –wire systems causes low system efficiency and poor power factor. The control strategies such as instantaneous active reactive power theory (p-q theory) are used for removing the problem of Neutral currents. Simulation results of current flowing through load neutral wire and its compensation by shunt neutral current is shown in Fig.25. The neutral current that may flow towards the transformer neutral point is effectively compensated so that the transformer neutral point is always at virtual zero potential which is shown in Fig.24.

*\*Address for correspondence:*

seepana\_2003@yahoo.co.in

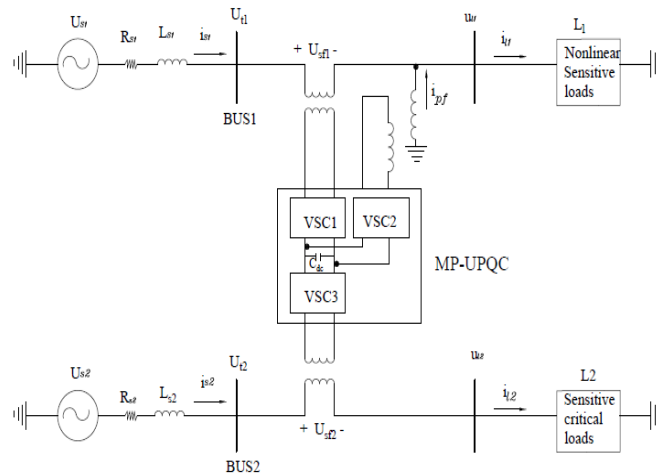


Fig.1. Typical MC-UPQC used in a distribution system

### MATHEMATICAL MODEL FOR PROPOSED SHUNT CONTROLLER METHODS

As shown in Fig. 1, the MC-UPQC consists of two series VSCs and one shunt VSC which are controlled independently. The switching control strategy for series VSCs and the shunt VSC are selected to be sinusoidal Pulse width-modulation (SPWM) voltage control and hysteresis current control, respectively. Details of the control algorithm, which are based on the  $d-q$  method [12] are shown below.

*Shunt-VSC*: functions of the shunt-VSC are:

- 1) To compensate for the reactive component of the load L1 current;
- 2) To compensate for the harmonic components of the load current;
- 3) To regulate the voltage of the common dc-link capacitor.

The measured load current ( $i_{l\_abc}$ ) is transformed into the synchronous  $dq0$  reference frame

$$\text{by using } i_{l\_dq0} = T_{abc}^{dq0} i_{l\_abc} \quad (1)$$

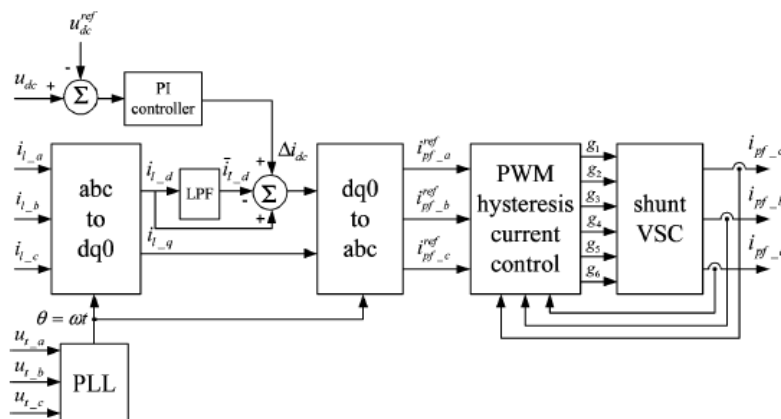


Fig.2. Shows the control block diagram for the shunt VSC

where the transformation matrix is shown in (2).

$$T_{abc}^{dq0} = \frac{2}{3} \begin{bmatrix} \cos(\omega t) & \cos(\omega t - 120^\circ) & \cos(\omega t + 120^\circ) \\ -\sin(\omega t) & -\sin(\omega t - 120^\circ) & -\sin(\omega t + 120^\circ) \\ \frac{1}{2} & \frac{1}{2} & \frac{1}{2} \end{bmatrix} \quad (2)$$

By this transformation, the fundamental positive-sequence component, which is transformed into dc quantities in the  $d$  and  $q$  axes, can be easily extracted by low-pass filters (LPFs). Also, all harmonic components are transformed into ac quantities with a fundamental frequency shift

$$i_{l_d} = \bar{i}_{l_d} + \hat{i}_{l_d} \tag{3}$$

$$i_{l_q} = \bar{i}_{l_q} + \hat{i}_{l_q} \tag{4}$$

Where  $i_{l_d}, i_{l_q}$  are  $d$ - $q$  components of load current,  $\bar{i}_{l_d}, \bar{i}_{l_q}$  are dc components, and  $\hat{i}_{l_d}, \hat{i}_{l_q}$  are the ac components of  $i_{l_d}$  and  $i_{l_q}$ .

If  $i_s$  is the feeder current and  $i_{pf}$  is the shunt VSC current and knowing  $i_s = i_l - i_{pf}$ , then  $d$ - $q$  components of the shunt VSC reference current are defined as follows:

$$i_{pf_d}^{ref} = \bar{i}_{l_d} \tag{5}$$

$$i_{pf_q}^{ref} = i_{l_q} \tag{6}$$

Consequently, the  $d$ - $q$  components of the feeder current are

$$i_{s_d} = \bar{i}_{l_d} \tag{7}$$

$$i_{s_q} = 0 \tag{8}$$

This means that there are no harmonic and reactive components in the feeder current. Switching losses cause the dc-link capacitor voltage to decrease. Other

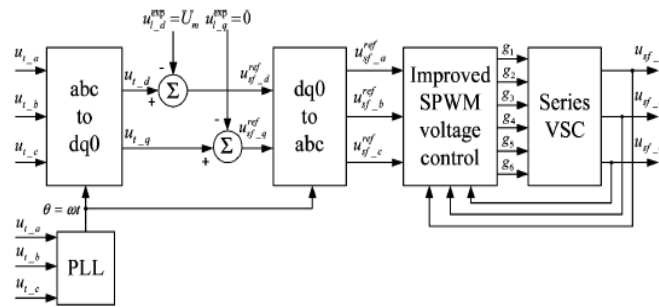


**Fig3.** Control block diagram of the series VSC

Disturbances, such as the sudden variation of the load, can also affect the dc link. In order to regulate the dc-link capacitor voltage, a proportional-integral (PI) controller is used as shown in Fig. 2. The input of the PI controller is the error between the actual capacitor voltage ( $u_{dc}$ ) and its reference value ( $u_{dc}^{ref}$ ). The output of the PI controller (i.e.,  $\Delta i_{dc}$ ) is added to the  $d$  component of the shunt-VSC reference current to form a new reference current as follows:

$$\begin{cases} i_{pf_d}^{ref} = \bar{i}_{l_d} + \Delta i_{dc} \\ i_{pf_q}^{ref} = i_{l_q} \end{cases} \tag{9}$$

As shown in Fig. 4, the reference current in(9) is then transformed back into the  $abc$  reference frame. By using PWM hysteresis current control, the output-compensating currents in each phase are obtained

$$i_{pf_{abc}}^{ref} = T_{dq0}^{abc} i_{pf_{dq0}}^{ref}; (T_{dq0}^{abc} = T_{abc}^{dq0-1}) \tag{10}$$

**Series-VSC:** Functions of the series VSCs in each feeder are:

- 1) To mitigate voltage sag and swell;
- 2) To compensate for voltage distortion, such as harmonics;
- 3) To compensate for interruption (in Feeder2 only).

The control block diagram of each series VSC is shown in Fig. 5. The bus voltage ( $u_{t_{abc}}$ ) is detected and then transformed into the synchronous  $dq0$  reference and then transformed into the synchronous  $dq0$  reference frame using

$$u_{t_{dq0}} = T_{abc}^{dq0} u_{t_{abc}} = u_{t1p} + u_{t1n} + u_{t10} + u_{t1h} \tag{11}$$

Where

$$\begin{cases} u_{t1p} = [u_{t1p_d} \ u_{t1p_q} \ 0]^T \\ u_{t1n} = [u_{t1n_d} \ u_{t1n_q} \ 0]^T \\ u_{t10} = [0 \ 0 \ u_{00}]^T \\ u_{th} = [u_{th_d} \ u_{th_q} \ u_{th_0}]^T \end{cases} \quad (12)$$

$u_{t1p}$ ,  $u_{t1n}$  and  $u_{t10}$  are fundamental frequency positive-, negative-, and zero-sequence components, respectively, and  $u_{th}$  is the harmonic component of the bus voltage.

According to control objectives of the MC-UPQC, the load voltage should be kept sinusoidal with a constant amplitude even if the bus voltage is disturbed. Therefore, the expected load voltage in the synchronous  $dq0$  reference frame ( $u_{l_{dq0}}^{exp}$ ) only has one value

$$u_{l_{dq0}}^{exp} = T_{abc}^{dq0} u_{l_{abc}}^{exp} = \begin{bmatrix} u_m \\ 0 \\ 0 \end{bmatrix} \quad (13)$$

Where the load voltage in the  $abc$  reference frame ( $u_{l_{abc}}^{exp}$ ) is

$$u_{l_{abc}}^{exp} = \begin{bmatrix} u_m \cos(\omega t) \\ u_m \cos(\omega t - 120^\circ) \\ u_m \cos(\omega t + 120^\circ) \end{bmatrix} \quad (14)$$

The compensating reference voltage in the synchronous  $dq0$  reference frame ( $u_{sf_{dq0}}^{ref}$ ) is defined as

$$u_{sf_{dq0}}^{ref} = u_{t_{dq0}} - u_{l_{dq0}}^{exp} \quad (15)$$

This means  $u_{t1p_d}$  in (12) should be maintained at  $U_m$  while all other unwanted components must be eliminated. The compensating reference voltages in (15) are then transformed back into the  $abc$  reference frame.

By using an improved SPWM voltage control technique (since PWM control with minor loop feedback) [8], the output compensation voltage of the series VSC can be obtained.

## PROPOSED SHUNT CONTROLLER METHOD USING p-q THEORY

The control algorithm for series active power filter (APF) is based on unit vector template generation scheme [12], whereas the control strategy for shunt APF is discussed in this section. Based on the load on the 3P4W system, the current drawn from the utility can be unbalanced. In this paper a new control strategy is proposed to compensate the current unbalance present in the load currents by expanding the concept of single phase p-q theory [10], [11]. According to this theory, a signal phase system can be defined as a pseudo two-phase system giving  $\pi/2$  lead or  $\pi/2$  lag, that is each phase voltage and current of the original three-phase system can be considered as three independent two phase systems. These resultant two phase systems can be represented in  $\alpha$ - $\beta$  coordinates, and thus, the p-q theory applied for balanced three phase system can also be used for each phase of unbalanced system independently. The actual load voltages and load currents are considered as  $\alpha$ -axis quantities where as the  $\pi/2$  lead load or  $\pi/2$  lag voltages and  $\pi/2$  lead or  $\pi/2$  lag load currents are considered as  $\beta$ -axis quantities. In this paper  $\pi/2$  lead is considered to achieve a two phase system for each phase. The major advantage of p-q theory is that it gives poor results under distorted and/or unbalanced input/utility voltages. In order to eliminate these limitations, the reference load voltage signals extracted for series APF are used instead of actual load voltages. For phase a, the load voltage and current in  $\alpha$ - $\beta$  coordinates can be represented by  $\pi/2$  lead

$$\begin{bmatrix} v_{La_\alpha} \\ v_{La_\beta} \end{bmatrix} = \begin{bmatrix} v_{La}^*(\omega t) \\ v_{La}^*(\omega t + \frac{\pi}{2}) \end{bmatrix} = \begin{bmatrix} v_{Lm} \sin(\omega t) \\ v_{Lm} \cos(\omega t) \end{bmatrix} \quad (16)$$

$$\begin{bmatrix} i_{La_\alpha} \\ i_{La_\beta} \end{bmatrix} = \begin{bmatrix} i_{La}(\omega t + \varphi L) \\ i_{La}[(\omega t + \varphi L) + \frac{\pi}{2}] \end{bmatrix} \quad (17)$$

Where  $v_{Lm}$  represents the desired load voltage magnitude and  $v_{La}^*(\omega t)$  depicts the reference load voltage. Similarly, the load voltage and current in  $\alpha$ - $\beta$  coordinates for phase b can be represented by  $\pi/2$  lead as

$$\begin{bmatrix} v_{Lb\_a} \\ v_{Lb\_b} \end{bmatrix} = \begin{bmatrix} v_{Lb}^*(\omega t) \\ v_{Lb}^*(\omega t + \frac{\pi}{2}) \end{bmatrix} = \begin{bmatrix} v_{Lm} \sin(\omega t - 120^\circ) \\ v_{Lm} \cos(\omega t - 120^\circ) \end{bmatrix} \quad (18)$$

$$\begin{bmatrix} i_{Lb\_a} \\ i_{Lb\_b} \end{bmatrix} = \begin{bmatrix} i_{La}(\omega t + \varphi L) \\ i_{La}[(\omega t + \varphi L) + \frac{\pi}{2}] \end{bmatrix} \quad (19)$$

In addition, the load voltage and current in  $\alpha$ - $\beta$  coordinates for phase c can be represented by  $\pi/2$  lead as

$$\begin{bmatrix} v_{Lc\_a} \\ v_{Lc\_b} \end{bmatrix} = \begin{bmatrix} v_{Lc}^*(\omega t) \\ v_{Lc}^*(\omega t + \frac{\pi}{2}) \end{bmatrix} = \begin{bmatrix} v_{Lm} \sin(\omega t + 120^\circ) \\ v_{Lm} \cos(\omega t + 120^\circ) \end{bmatrix} \quad (20)$$

$$\begin{bmatrix} i_{Lc\_a} \\ i_{Lc\_b} \end{bmatrix} = \begin{bmatrix} i_{Lc}(\omega t + \varphi L) \\ i_{Lc}[(\omega t + \varphi L) + \frac{\pi}{2}] \end{bmatrix} \quad (21)$$

By using the definition of three phase p-q theory, for balanced three-phase system, the instantaneous power components can be depicted as

Instantaneous active power

$$p_{L,abc} = v_{L,abc\_a} \cdot i_{L,abc\_a} + v_{L,abc\_b} \cdot i_{L,abc\_b} \quad (22)$$

$$\text{Instantaneous reactive power } q_{L,abc} = v_{L,abc\_a} \cdot i_{L,abc\_b} - v_{L,abc\_b} \cdot i_{L,abc\_a} \quad (23)$$

Assuming the phase a, the phase-a instantaneous load active and instantaneous load reactive powers can be represented by

$$\begin{bmatrix} p_{La} \\ q_{La} \end{bmatrix} = \begin{bmatrix} v_{La\_a} & v_{Lb\_b} \\ -v_{Lb\_b} & v_{La\_a} \end{bmatrix} \begin{bmatrix} i_{La\_a} \\ i_{La\_b} \end{bmatrix} \quad (24)$$

Where

$$p_{La} = \bar{p}_{La} + \tilde{p}_{La} \quad (25)$$

$$q_{La} = \bar{q}_{La} + \tilde{q}_{La} \quad (26)$$

$\bar{p}_{La}$  and  $\bar{q}_{La}$  represent the DC elements which are responsible for fundamental load active and reactive powers, whereas  $\tilde{p}_{La}$  and  $\tilde{q}_{La}$  depicts the ac components which are in equations 25 and 26, controllable for harmonic powers. The phase-a fundamental instantaneous load active and reactive power elements can be extracted from  $p_{La}$  and  $q_{La}$  respectively by using a low pass filter.

Therefore, the instantaneous fundamental load active power for phase-a is given by

$$p_{La,1} = \bar{p}_{La} \quad (27)$$

and Instantaneous fundamental load reactive power for phase-a is given by

$$q_{La,1} = \bar{q}_{La} \quad (28)$$

Similarly the fundamental instantaneous load active and the fundamental instantaneous load reactive powers for phases-b and c can be evaluated as

Instantaneous fundamental load active power for phase b

$$p_{Lb,1} = \bar{p}_{Lb} \quad (29)$$

Instantaneous fundamental load reactive power for phase b

$$q_{Lb,1} = \bar{q}_{Lb} \quad (30)$$

Instantaneous fundamental load active power for phase c

$$p_{Lc,1} = \bar{p}_{Lc} \quad (31)$$

Instantaneous fundamental load reactive power for phase c

$$q_{Lc,1} = \bar{q}_{Lc} \quad (32)$$

Since the load current drawn by each phase is different due to different loads which may be present inside plant, therefore the instantaneous fundamental load reactive power and the instantaneous fundamental load active power demand for each phase may not be the same. In order to make this load unbalanced power demand to balanced fundamental three phase active power, the unbalanced load power should be properly redistributed between utility to get the linear and balanced loads.

The unbalanced or balanced reactive power demanded by the load will be handled by a shunt APF. The aforementioned task is obtained by summing instantaneous load active power demands of all the three phases and redistributing it again on each utility phase that is from equations (27), (29) and (31).

$$p_{L,Total} = p_{La,1} + p_{Lb,1} + p_{Lc,1} \quad (33)$$

$$p_{S/ph}^* = (p_{L,Total})/3 \quad (34)$$

Equation (34) gives the distributed per phase fundamental active power demand that each phase of utility supplies in order to obtain perfect balanced source currents. It is clear that under all the conditions the total fundamental active power demand by the loads would be equal to the total power drawn from the utility but with exactly balanced way even though the load currents are unbalanced. Thus the reference compensating currents representing a perfectly balanced 3-phase system can be extracted by taking the inverse of (24).

$$\begin{bmatrix} i_{Sa\_a}^* \\ i_{Sa\_b}^* \end{bmatrix} = \begin{bmatrix} v_{La\_a} & v_{La\_b} \\ -v_{La\_b} & v_{La\_a} \end{bmatrix}^{-1} \cdot \begin{bmatrix} p_{S/ph}^* + p_{dc/ph} \\ 0 \end{bmatrix} \quad (35)$$

In equation (35),  $p_{dc/ph}$  is the precise amount of per-phase active power that should be taken from the source in order to maintain the dc-link voltage at a constant level and to overcome the losses related with MC-UPQC. The oscillating instantaneous active power  $\tilde{p}_{La}$  should be exchanged between the load and shunt APF. The reactive power term  $q_{La}$  in equation (35) is assumed as zero since the utility would not supply load reactive power demand. In the above matrix, the  $\alpha$ -axis reference compensating current depicts the current that is at  $\frac{\pi}{2}$  lead with respect to the original system.

Therefore,

$$i_{Sa}^*(t) = \{v_{La\_a}(t)/v_{La\_a}^2 + v_{La\_b}^2\} \cdot \{p_{S/ph}^*(t) + p_{dc/ph}^*(t)\} \quad (36)$$

Similarly the reference source currents for phases b can be measured as

$$i_{Sb}^*(t) = \{v_{Lb\_a}(t)/(v_{Lb\_a}^2 + v_{Lb\_b}^2)\} \cdot \{p_{S/ph}^*(t) + p_{dc/ph}^*(t)\} \quad (37)$$

$$i_{Sc}^*(t) = \{v_{Lc\_a}(t)/(v_{Lc\_a}^2 + v_{Lc\_b}^2)\} \cdot \{p_{S/ph}^*(t) + p_{dc/ph}^*(t)\} \quad (38)$$

The reference neutral current signal can be extracted by simply adding all the sensed load currents without actual neutral current sensing as

$$i_{L\_n}(t) = i_{La}(t) + i_{Lb}(t) + i_{Lc}(t) \quad (39)$$

$$i_{Sh\_n}^*(t) = -i_{L\_n}(t) \tag{40}$$

The proposed balanced per-phase fundamental active power estimation, dc link voltage control loop related with PI regulator, the reference source current generation are given in the equations (36) to (38) and the reference neutral current generations are shown in Fig. 4(a) - (d) respectively.

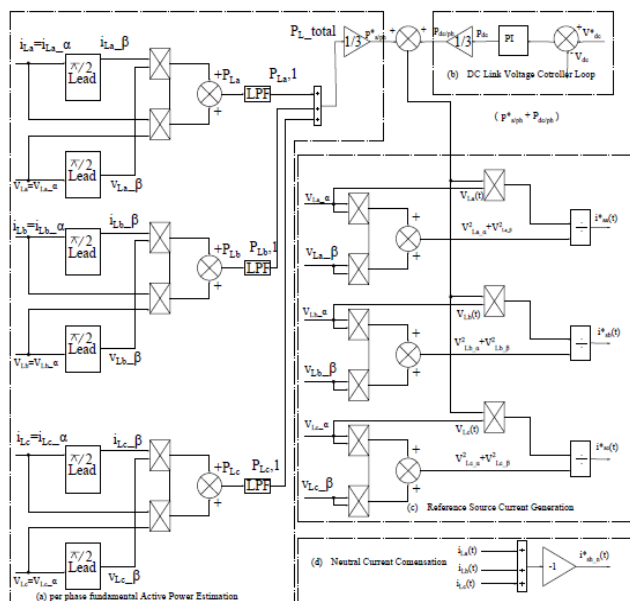


Fig4. Shunt active filter Control block diagram

(a)proposed balanced per-phase fundamental active power estimation. (b) DC-link voltage control loop. (c) Reference source current generation. (d) Neutral current compensation.

### SIMULATION RESULTS

The proposed MC-UPQC and its Neuro-fuzzy control schemes have been tested through extensive case study simulations using MATLAB/SIMULINK. In this section, simulation results are presented, and the performance of the proposed MC-UPQC system is shown. Simulation is carried out in this case study under distorted conditions of current and supply voltages in feeder1. The distorted non-linear load currents are compensated very well. The input voltage harmonics and current harmonics caused by non-linear load, effectiveness of MCUPQC with different controllers is evident from Fig.8, Fig 9 & Fig.10. As the source current becomes sinusoidal and balanced from 0.5 s. The scheme is first simulated without MC-UPQC to find out the THD of the supply voltage and current. Then, it is simulated with MC-UPQC to observe the difference in THD of supply current and voltages for the proposed model MC-UPQC.

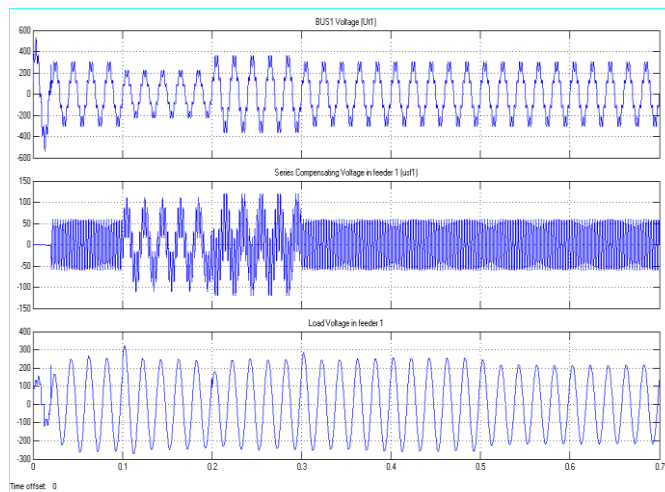
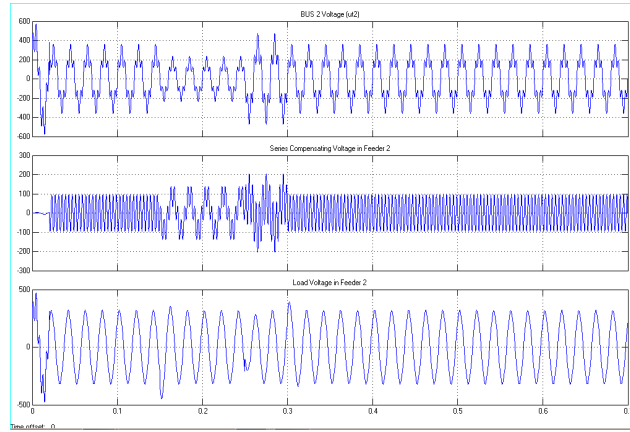
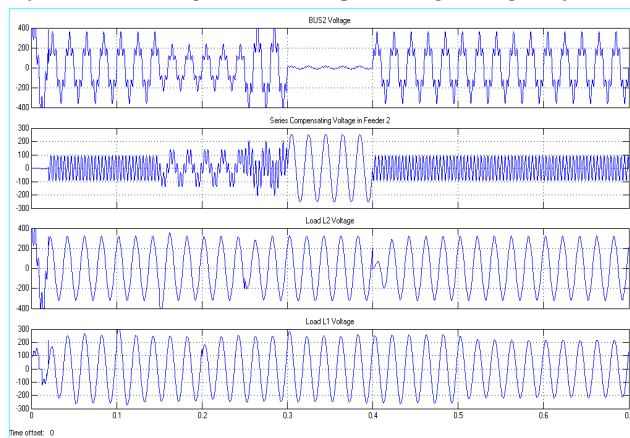


Fig5. simulated results for bus1 voltage, its series compensating voltage and load voltage in Feeder 1



**Fig6.** Simulated results for BUS2 voltage, series compensating voltage in feeder 2, and its load voltage



**Fig7.** simulated results for BUS2 Voltage under fault condition, its Series compensation Voltage in feeder 2

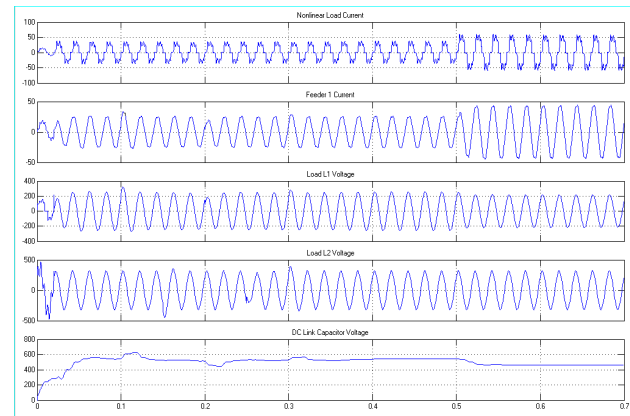


**Fig8.** Simulation results: Nonlinear load current, Feeder1 current, load L1, L2 voltages and DC-link capacitor voltage for load change with PI controller

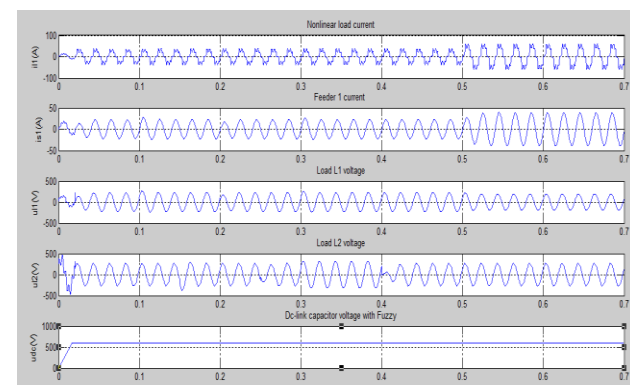


**Fig9.** Simulation results for: Nonlinear load current, Feeder1 current, load L1, L2 voltages and DC-link capacitor voltage when load change with FUZZY controller



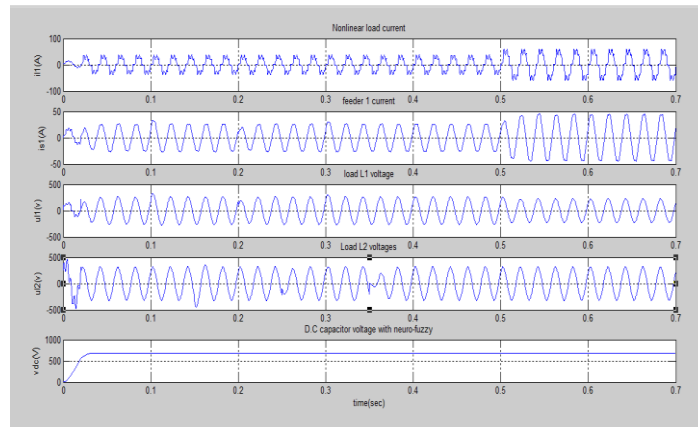


**Fig10.** Simulation results: Nonlinear load current, Feeder1 current, load L1, L2 voltage and DC-link capacitor voltage for load change with NEURO-FUZZY controller

Let us consider that the power system in Fig.1 consists of two three-phase three-wire 380(v) (rms, L-L), 50-Hz utilities. The BUS1 voltage ( $u_{t1}$ ) contains the seventh-order harmonic with a value of 22%, and the BUS2 voltage ( $u_{t2}$ ) contains the fifth-order harmonic with a value of 35%. The BUS1 voltage contains 25% sag between  $0.1 \text{ s} < t < 0.2 \text{ s}$  and 20% swell between  $0.2 \text{ s} < t < 0.3 \text{ s}$ . The BUS2 voltage contains 35% sag between  $0.15 \text{ s} < t < 0.25 \text{ s}$  and 30% swell between  $0.25 \text{ s} < t < 0.3 \text{ s}$ . The nonlinear/sensitive load L1 is a three-phase rectifier load which supplies an RC load of  $10\Omega$  and  $30 \mu\text{F}$ . Finally, the critical load L2 contains a balance RL load of  $10 \Omega$  and  $100\text{mH}$ .

The MC-UPQC is switched on at  $t = 0.02 \text{ s}$ . The BUS1 voltage, the corresponding compensation voltage injected by VSC1 and finally load L1 voltage are shown in Fig. 7. In all figures, only the phase *a* waveform is shown for simplicity.

Similarly, the BUS2 voltage, the corresponding compensation voltage injected by VSC3, and finally, the load L2 voltage are shown in Fig.8. As shown in these figures, distorted voltages of BUS1 and BUS2 are satisfactorily compensated for across the loads L1 and L2 with very good dynamic response.

The nonlinear load current, its corresponding compensation current injected by VSC2, compensated Feeder1 current, and, finally, the dc-link capacitor voltage are shown in Fig. 10. The distorted nonlinear load current is compensated very well, and the total harmonic distortion (THD) of the feeder current is reduced from 22% to less than 5%. Also, the dc voltage regulation loop has functioned properly under all the disturbances, such as sag/swell in both feeders One of the many solutions is the use of a combined system of shunt and Series converter like multi converter unified power quality conditioner (MC-UPQC) .compensate the supply voltage and the load current or to mitigate any type of voltage and current fluctuations sag, swell and power factor correction in a power distribution network. The controllers used here are based on PI, Fuzzy and Neuro-Fuzzy controllers of the MC-UPQC in detail. The control strategies are modeled using MATLAB/SIMULINK. The simulation results are listed in comparison of different controllers are shown in figures 8,9and 10.

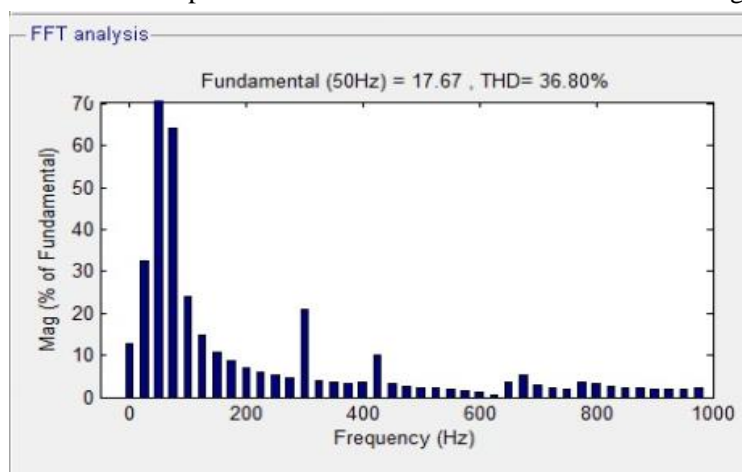


**Fig11.** THD for utility side voltage without MC-UPQC

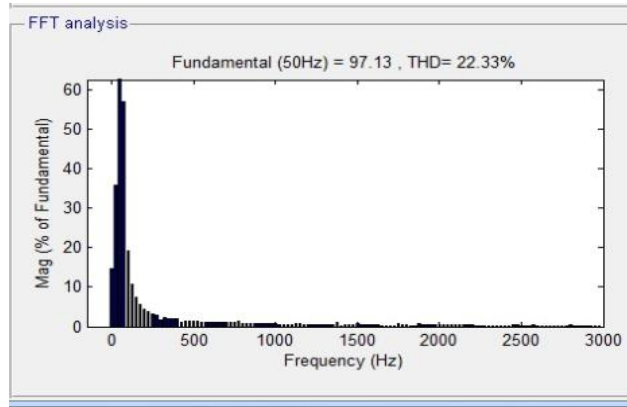


Fig12. THD for utility side current without MC-UPQC

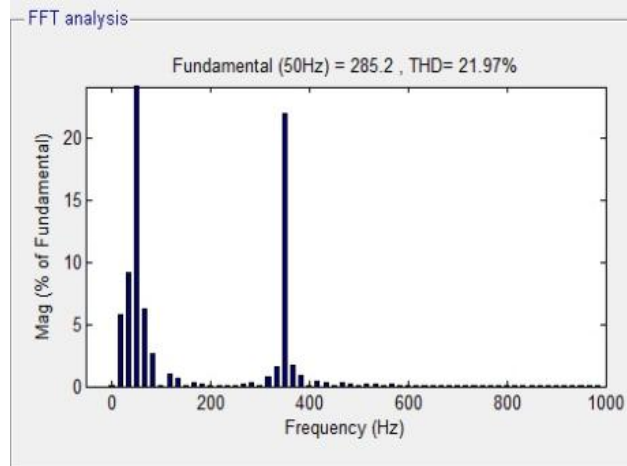


Fig13. THD for utility side voltage using PI controller with MC-UPQC (with d-q method)

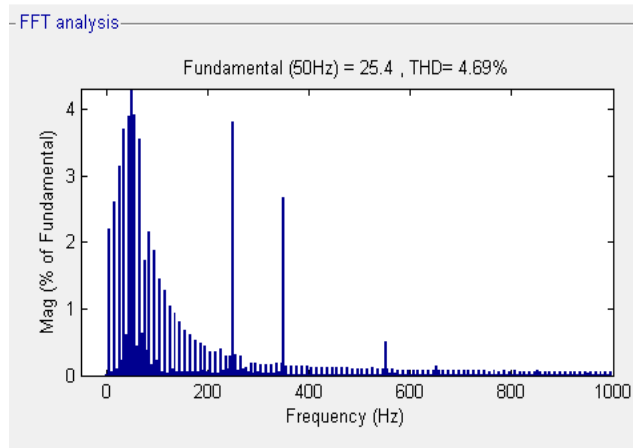


Fig14. THD for utility side current using PI controller with MC-UPQC (with d-q method)

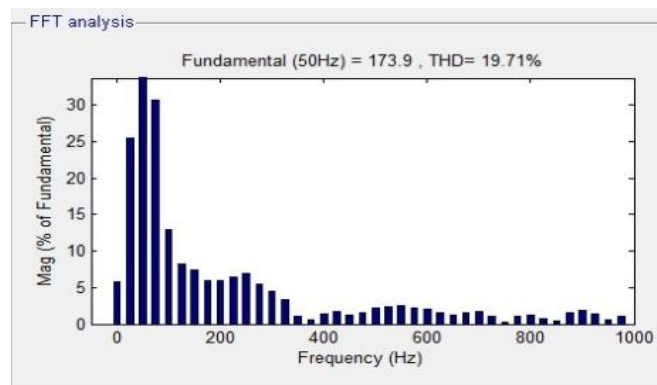


Fig15. THD for utility side voltage with FUZZY controller using MC-UPQC (with d-q method)

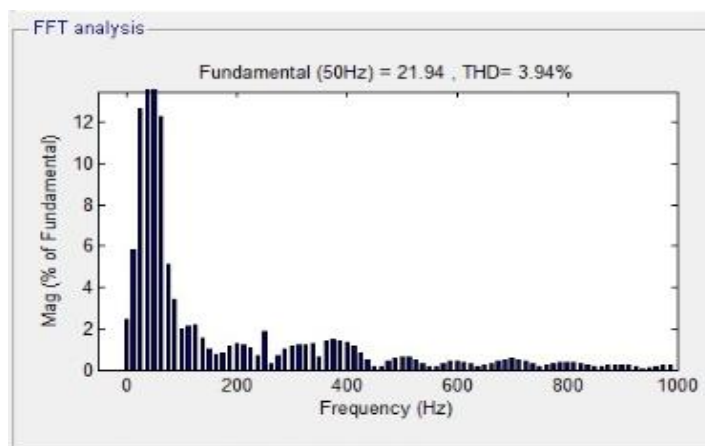


Fig16. THD for utility side current with FUZZY controller using MC-UPQC (with d-q method)

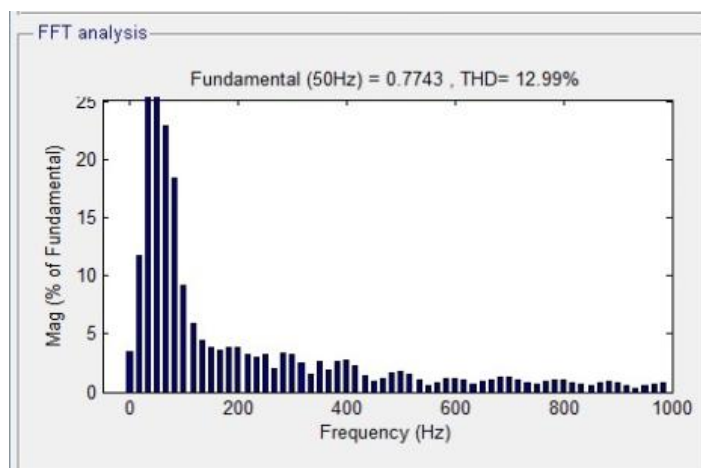


Fig17. THD for utility side voltage using NEURO-FUZZY controller with MC-UPQC (with d-q method)

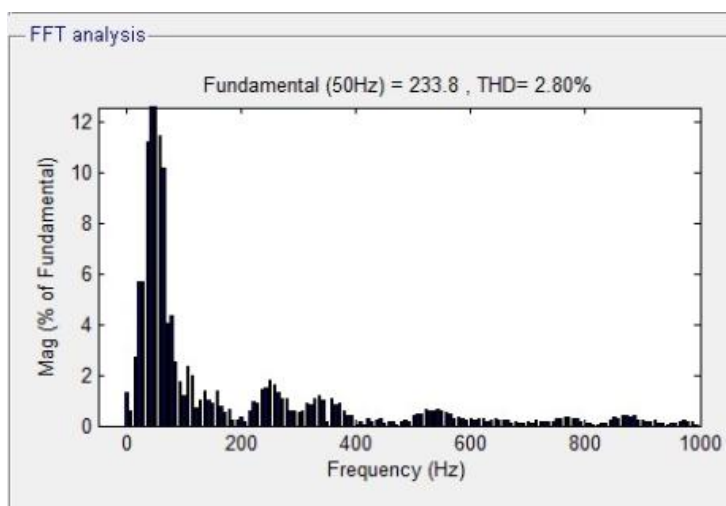
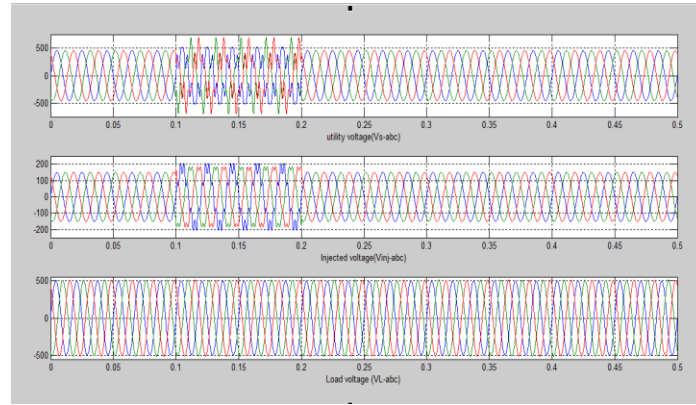


Fig18. THD for utility side current using NEURO-FUZZY controller with MC-UPQC (with d-q method)

### PROPOSED 3P4W MC-UPQC STRUCTURE STUDIES

The supply voltages of the two feeders consists of two three-phase three wire , The BUS1 voltage ( $u_{11}$ ) contains the seventh-order harmonic with a value of 22%, and the BUS2 voltage ( $u_{12}$ ) contains the fifth order harmonic feeder1 load is a combination of a three-phase R-L load ( $R = 10$  Ohms,  $L = 30\mu$  H) and a three-phase diode bridge rectifier followed by R-L load on dc side ( $R = 10$  Ohms,  $L = 100$  mH) which draws harmonic current. Similarly to introduce distortion in supply voltages of feeder2, 7th and 5th harmonic voltage sources, which are 22% and 35% of fundamental input supply voltages are connected in series with the supply voltages VSC1 and VSC3 respectively. In order to demonstrate the performance of the proposed model of MC-UPQC simulation case studies are carried out.



**Fig19.** (i).Simulation result of Utility voltage ( $V_{S\_abc}$ ), (ii). Injected voltage ( $V_{inj\_abc}$ ), (iii).Load voltage ( $V_{L\_abc}$ ) during swell condition

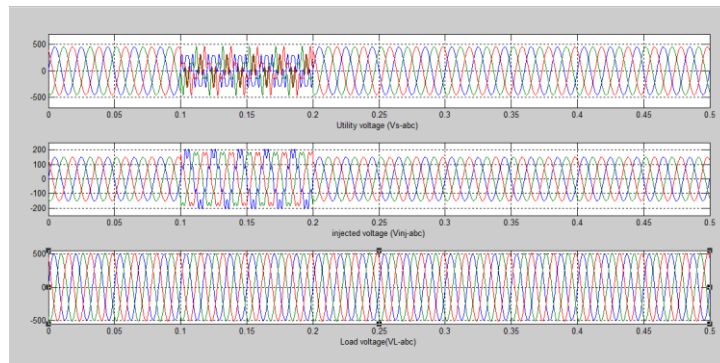


**Fig20.** (i).Simulation result of Utility voltage ( $V_{S\_abc}$ ), (ii). Injected voltage ( $V_{inj\_abc}$ ), (iii). Load voltage ( $V_{L\_abc}$ ) during sag condition .

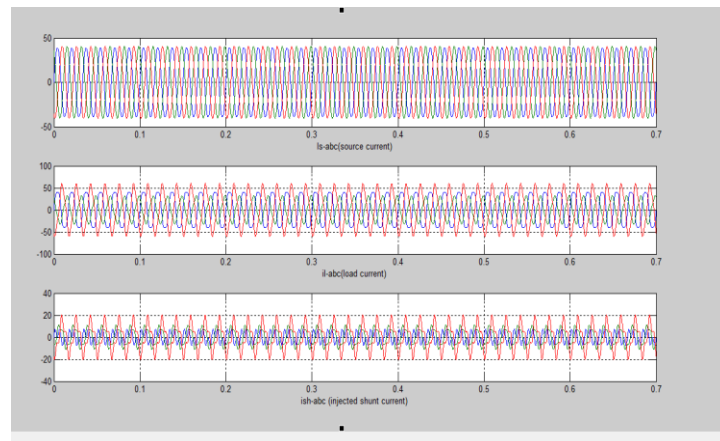


**Fig21.** (i).Simulation results of a Source current ( $iS\_abc$ ), (ii)Load current ( $iL\_abc$ ) (iii).Shunt compensating current ( $iSh\_abc$ ).

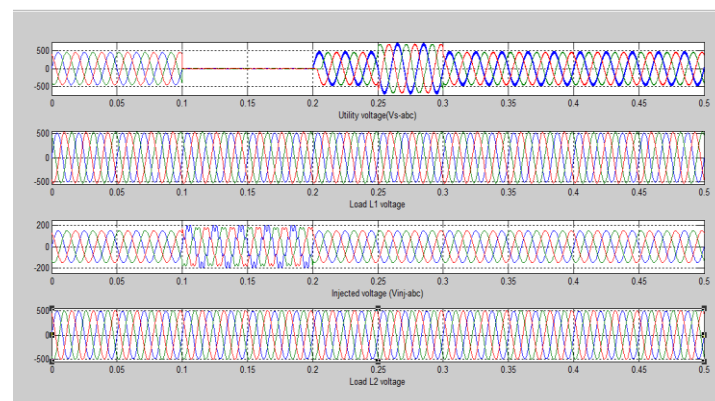


**Fig22.** (i).Simulation results for an upstream fault and swell condition on Feeder2, (ii)load L1 voltage,(iii)compensating voltage(iv) load L2 voltages.

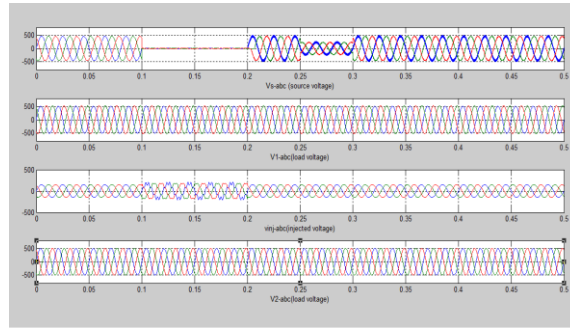


Fig23. (i).Simulation results for an upstream fault and sag condition on Feeder2, (ii)load L1 voltage,(iii)compensating voltage(iv) load L2 voltages.

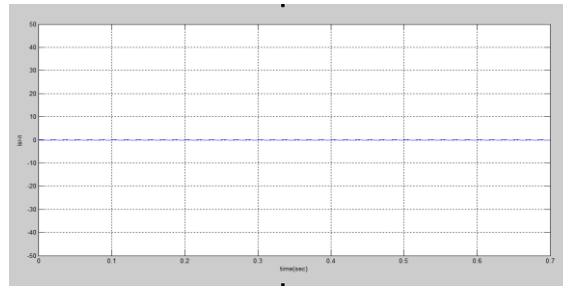


Fig.24.Simulation result of Neutral current flowing towards series transformer ( $i_{Sr_n}$ ).

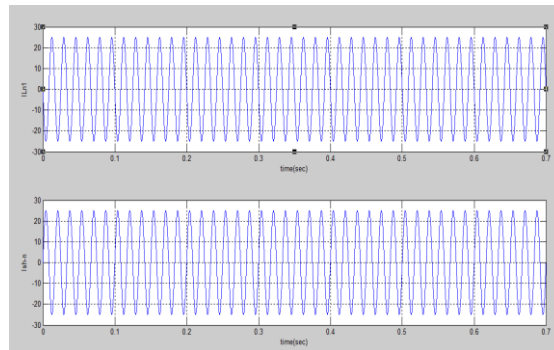


Fig25. (i)Simulation results of Current flowing through load neutral wire ( $i_{L_n}$ )(ii)Shunt neutral compensating current ( $i_{Sh_n}$ ).

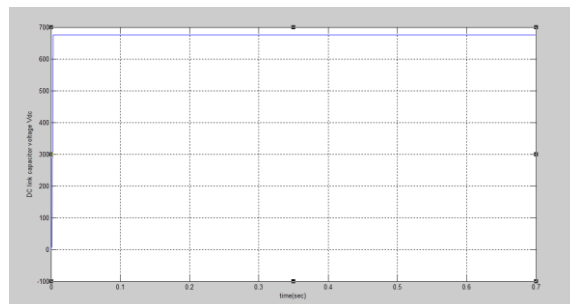


Fig26. Simulation results of a DC-link capacitor voltage ( $v_{dc}$ ).

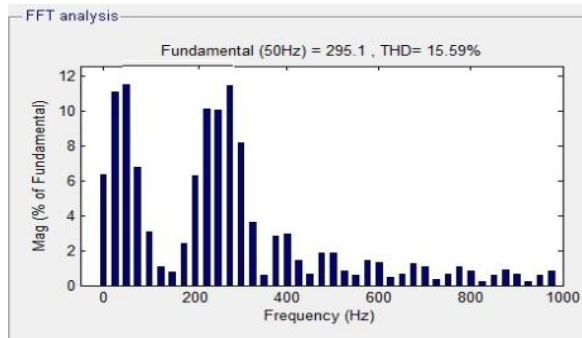


Fig27.THd for utility side voltage without MC-UPQC

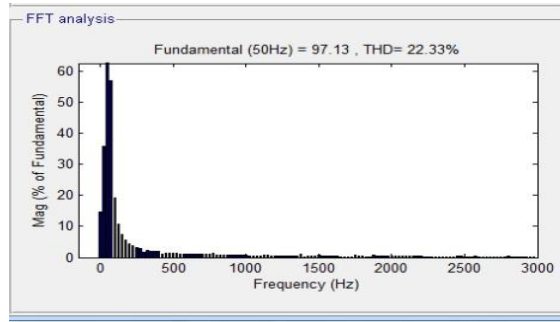


Fig28. THD for utility side current without MC-UPQC

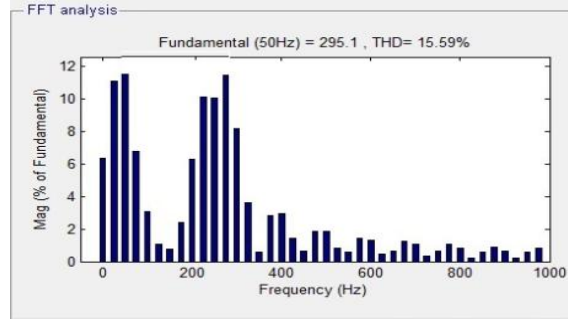


Fig29. THD for utility side voltage using PI controller with MC-UPQC (with p-q theory)

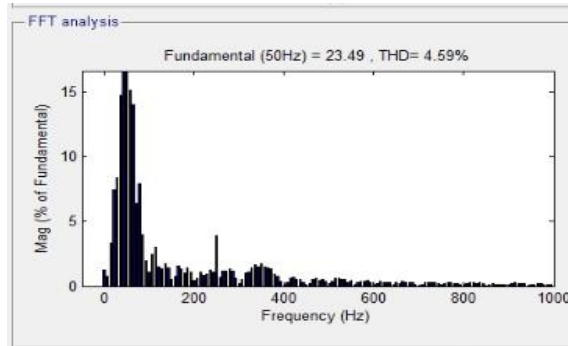


Fig30. THD for utility side current using PI controller with MC-UPQC (with p-q theory).

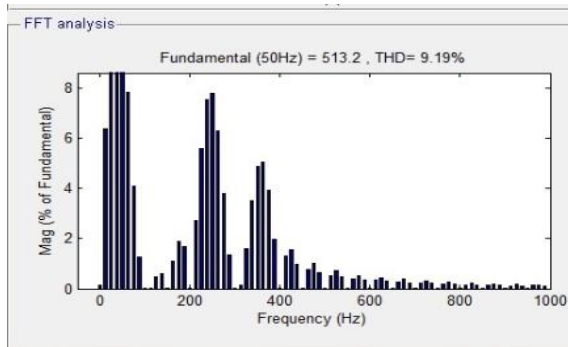


Fig31. THD for utility side voltage using FUZZY controller with MC-UPQC (with p-q theory)

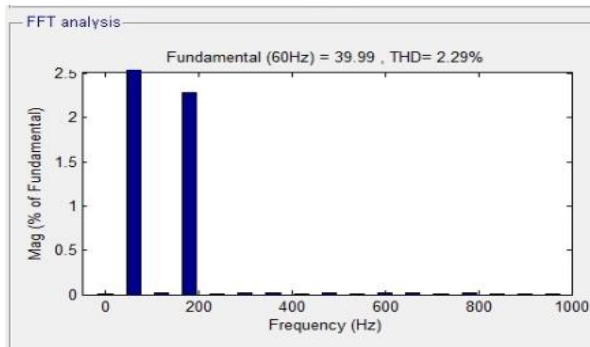


Fig32. THD for utility side current using FUZZY controller with MC-UPQC (with p-q theory)

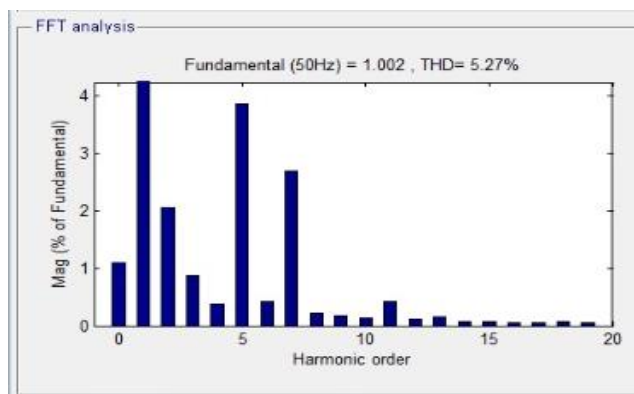


Fig32. THD for utility side voltage using NEURO-FUZZY controller with MC-UPQC (with p-q theory)

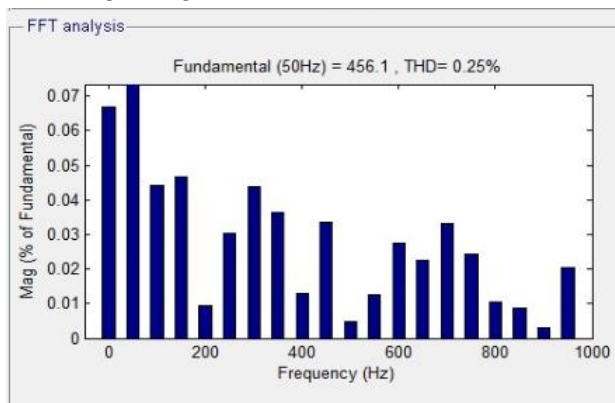


Fig33. THD for utility side current using NEURO-FUZZY controller with MC-UPQC (with p-q theory).

Table1. Comparison table for Voltage and current harmonics (THDs) of MC-UPQC

Controller used	THD values % using dq method	THD values % using p-q theory
Without MC-UPQC utility side voltage	36.805	36.805
Without MC-UPQC utility side current	22.33	22.33
MC-UPQC with PI controller utility side voltage	21.97	15.59
MC-UPQC with PI controller utility side current	4.69	4.59
MC-UPQC with FUZZY controller utility side voltage	19.71	9.19
MC-UPQC with FUZZY controller utility side current	3.94	2.29
MC-UPQC with NEURO-FUZZY controller utility side voltage	12.99	5.27
MC-UPQC with NEURO-FUZZY controller utility side current	2.80	0.25

## CONCLUSION

A custom power device called MC-UPQC is used to mitigate voltage and current harmonics, to improve voltage regulation and to compensate reactive power. The simulation results on a two-feeder and multi bus distribution system are established by compensating execution of a novel series and shunt compensator. By increasing the number of VSCs, the advanced MC-UPQC can achieve various compensation functions. The compensation is shown by using PI, FUZZY and NEURO-FUZZY controllers. A relevant mathematical calculation has been characterized constituting the fact that in both the cases with and without MC-UPQC using d-q method and p-q theory. The response of NEURO-FUZZY controller with p-q theory has been shown better results in the minimization of THD's in case of voltage and current which are observed from the table.1.

## REFERENCES

- [1] Hamid Reza Mohammadi, Ali Yazdian Varjani, and Hossein Mokhtari, “Multiconverter Unified Power-Quality Conditioning System: MC-UPQC” IEEE TRANSACTIONS ON POWER DELIVERY, VOL. 24, NO. 3, JULY 2009.
- [2] R.Rezaeipour and A.Kazemi, “Review of Novel control strategies for UPQC” Internal Journal of Electric and power Engineering 2(4) 241-247, 2008.
- [3] S.Ravi Kumar and S.Siva Nagaraju “Simulation of STATCOM and DVR in power systems” Vol. 2, No. 3, June 2007 ISSN 1819-6608 ARPN Journal of Engineering and Applied Sciences.

- [4] M.V.Kasuni Perera “Control of a Dynamic Voltage Restorer to compensate single phase voltage sags” Master of Science Thesis, Stockholm, Sweden 2007.
- [5] M. Basu, S. P. Das, and G. K. Dubey, “Comparative evaluation of two models of UPQC for suitable interface to enhance power quality,” *Elect.Power Syst. Res.*, pp. 821–830, 2007.
- [6] A. K. Jindal, A.Ghosh, and A. Joshi, “Interline unified power quality conditioner,” *IEEE Trans. Power Del.*, vol. 22, no. 1, pp. 364–372, Jan. 2007.
- [7] B. Singh, K. Al-Haddad, and A.Chandra, “A review of active power filters for power quality improvement,” *IEEE Trans. Ind. Electron.*, vol. 45,no. 5, pp. 960–971, Oct. 1999.
- [8] C. A. Quinn and N.Mohan, “Active filtering of harmonic currents in three-phase, four-wire systems with three-phase and single-phase nonlinear loads,” in *Proc. 7th IEEE APEC*, 1992, pp. 829–836.
- [9] H. Akagi, Y. Kanazawa, and A. Nabae, “Instantaneous reactive power compensators comprising switching devices without energy storage components,”*IEEE Trans. Ind. Appl.*, vol. IA-20, no. 3, pp. 625–630,May/Jun. 1984.
- [10] Y. Komatsu and T. Kawabata, “A control method of active power filter in unsymmetrical and distorted voltage system,” in *Proc. Conf. IEEE Power Convers.*, 1997, vol. 1, pp. 161–168.
- [11] M. T. Haque, “Single-phase PQ theory,” in *Proc. 33rd IEEE PESC*, 2002, vol. 4, pp. 1815–1820.
- [12] J. M. Correa, S. Chakraborty, M. G. Simoes, and F. A. Farret, “A singlephase high frequency AC microgrid with an unified power quality conditioner,” in *Conf. Rec. 38th IEEE IAS Annu. Meeting*, 2003, vol. 2,pp. 956–962.
- [13] V. Khadkikar, A. Chandra, A. O. Barry, and T. D. Nguyen, “Application of UPQC to protect a sensitive load on a polluted distribution network,”in *Proc. IEEE PES General Meeting*, Montreal, QC, Canada, 2006, 6 pp.
- [14] V. Khadkikar, A. Chandra, A. O. Barry, and T. D. Nguyen, “Conceptual analysis of unified power quality conditioner (UPQC),” in *Proc. IEEE ISIE*, 2006, pp. 1088–1093.
- [15] Kishore Chatterjee, B.G. Fernandes, and Gopal K.Dubey, An Instantaneous Reactive Volt Ampere Compensator and Harmonic Suppressor System, *IEEE Trans. Power Electronics*,vol. 14, no.2, Mar.1999, pp. 381-392.
- [16] M. Rastogi, R. Naik, and N. Mohan, “A comparative evaluation of harmonic reduction techniques in three-phase utility interface of power electronic loads,” *IEEE Trans. Ind. Appl.*, vol. 30, no. 5, pp. 1149–1155, Sep./Oct. 1994.
- [17] B.M. Bird, J.F. Marsh, and P.R. McLellan, “Harmonic reduction in multiple converters by triple-frequency current injection”, *IEEE Proc. 116 (10), 1730–1734 (1969)*.
- [18] H. Sasaki and T. Machida, “A new method to eliminate ac harmonic currents by magnetic compensation - consideration on basic design”, *IEEE Trans. Power Appl. Syst.* 90 (5), 2009–2019 (1971).
- [19] M. J. Newman, D. G. Holmes, J. G. Nielsen and F. Blaabjerg, “A dynamic voltage restorer (DVR) with selective harmonic compensation at medium voltage level”, *IEEE Trans. Ind. Application*, vol. 41, issue 6, Nov.-Dec. 2005, pp. 1744-1753.

## **AUTHORS’ BIOGRAPHY**



**B. Rajani** received B.Tech degree in Electrical & Electronics Engineering from S.I.S.T.A.M college of Engineering, Srikakulam 2002 and M.E degree in Power Systems and Automation from Andhra University, Visakhapatnam in the year 2008. she presently is working towards her Ph.D degree in S.V. University, Tirupathi. Her areas of interest are in power systems operation & control and power quality improvement.



**Dr.P.Sangameswararaju** received Ph.D from Sri Venkateswara University, Tirupathi, Andhra Pradesh. Presently he is working as professor in the department of Electrical & Electronics Engineering, S.V. University. Tirupati, Andhra Pradesh. He has about 70 publications in National and International Journals and conferences to his credit. His areas of interest are in power system operation & control and stability